electronic reprint

Journal of
Synchrotron Radiation
ISSN 0909-0495

Determination of nanostructure of liposomes containing two model drugs by X-ray scattering from a synchrotron source

Alexandr Nasedkin, Jan Davidsson and Mont Kumpugdee-Vollrath

J. Synchrotron Rad. (2013). **20**, 721–728

Copyright © International Union of Crystallography

Author(s) of this paper may load this reprint on their own web site or institutional repository provided that this cover page is retained. Republication of this article or its storage in electronic databases other than as specified above is not permitted without prior permission in writing from the IUCr.

For further information see http://journals.iucr.org/services/authorrights.html

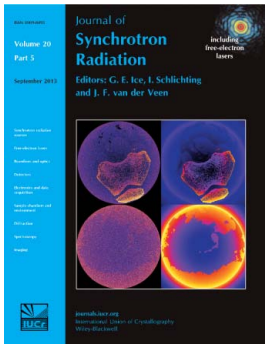

Synchrotron radiation research is rapidly expanding with many new sources of radiation being created globally. Synchrotron radiation plays a leading role in pure science and in emerging technologies. The *Journal of Synchrotron Radiation* provides comprehensive coverage of the entire field of synchrotron radiation research including instrumentation, theory, computing and scientific applications in areas such as biology, nanoscience and materials science. Rapid publication ensures an up-to-date information resource for scientists and engineers in the field.

Crystallography Journals Online is available from **journals.iucr.org**

Journal of
Synchrotron
Radiation

ISSN 0909-0495

Received 4 January 2013
Accepted 20 July 2013

Determination of nanostructure of liposomes containing two model drugs by X-ray scattering from a synchrotron source

Alexandr Nasedkin,[a] Jan Davidsson[a] and Mont Kumpugdee-Vollrath[b]*

[a]Department of Chemistry, Ångström Laboratory, Uppsala University, Lagerhyddsvägen 1, S-75120 Uppsala, Sweden, and [b]Department of Pharmaceutical Engineering, Faculty of Mathematics-Physics-Chemistry, Beuth Hochschule für Technik Berlin, University of Applied Sciences, Luxemburger Strasse 10, Berlin 13353, Germany. E-mail: vollrath@beuth-hochschule.de

Small-angle X-ray scattering has been employed to study how the introduction of paracetamol and acetylsalicylic acid into a liposome bilayer system affects the system's nanostructure. An X-ray scattering model, developed for multilamellar liposome systems [Pabst *et al.* (2000), *Phys. Rev. E*, **62**, 4000–4009], has been used to fit the experimental data and to extract information on how structural parameters, such as the number and thickness of the bilayers of the liposomes, thickness of the water layer in between the bilayers, size and volume of the head and tail groups, are affected by the drugs and their concentration. Even though the experimental data reveal a complicated picture of the drug–bilayer interaction, they clearly show a correlation between nanostructure, drug and concentration in some aspects. The localization of the drugs in the bilayers is discussed.

© 2013 International Union of Crystallography
Printed in Singapore – all rights reserved

Keywords: SAXS; WAXS; acetylsalicylic acid; paracetamol; drug-loaded liposomes.

1. Introduction

Liposomes have been widely used in the pharmaceutical field as drug delivery systems for many years now. The use of such systems is associated with a more efficient release of a drug to the target which in turn will reduce the overall toxicity (Molema & Meijer, 2001; Torchilin & Weissig, 2003; Saag & Dismukes, 1988; Ulrich, 2002). Most liposomes are prepared from phospholipids and can take unilamellar or multilamellar forms with different phases, *e.g.* gel, liquid crystalline or hexagonal phases (Seddon *et al.*, 2009). Liposomes are unique objects exhibiting quasi-long-range order regarding their structure.

The repetitive structure and precise bilayer profile could be recovered from the X-ray scattering pattern (Pabst *et al.*, 2000; Nagle & Tristram-Nagle, 2000). The X-ray scattering technique represents a powerful tool for structural investigations (Putnam *et al.*, 2007) since it provides a direct sampling of the real structure of the object. Nuclear magnetic resonance (NMR) is also advantageous in this respect, but is restricted to local structures. Förster resonance energy transfer, another commonly used technique, only monitors the distance between two specific chromophores.

The introduction of drugs into liposomes is not straightforward and will involve several chemical and physical obstacles that may affect the stability and efficiency of the system. The localization of a drug in a liposome is important and will affect the liposomes ability to carry and release the drug. For this reason it is important to understand the interaction between a drug and a liposome in detail. Such knowledge will help in the preparation of suitable systems and to better understand its pharmacological consequences. This issue has been addressed previously by different experimental techniques such as infrared spectroscopy (Casal *et al.*, 1987), NMR (Seydel & Wiese, 2002), UV–VIS spectroscopy (Custódio *et al.*, 1991), differential scanning calorimetry (Heerklotz, 2004), circular dichroism spectroscopy (Gallois *et al.*, 1998) or X-ray scattering (Barrett *et al.*, 2012). A drug may change the local properties of the surrounding water, for instance by changing its pH value. This could cause a change in the structure of liposomes inducing a reorganization of lipid bilayer and even destabilization of the whole system (Drummond *et al.*, 2000). The drug may also be adsorbed to the bilayer surface or, alternatively, even penetrate into the hydrophobic core, which can significantly affect the properties of the phospholipid membrane. For example, models developed by Castorph and colleagues (Castorph *et al.*, 2010) take physisorbed proteins to the bilayer surface into account.

In this study, the focus is on the structure of liposomes prepared from commercially available natural phospholipids like Phospholipon® 90G, 90NG, 85G. All three products contain phosphatidylcholines (PCs) as the major constituent (>85 wt%) with minor admixture of lysophosphatidylcholines (LPCs) (3–6 wt%) and with insignificant amounts of toco-

electronic reprint

Table 1
Composition of different commercial phospholipids.

	PL 85G	PL 90G	PL 90NG
Phosphatidylcholine (wt%)	Minimum 85	94–102	Minimum 90
Lysophosphatidylcholine (wt%)	3 ± 3	Maximum 4	Maximum 6
α-Tocopherol (wt%)	0	Maximum 0.3	Maximum 0.3
Ethanol (wt%)	Maximum 0.5	Maximum 0.2	Maximum 0.5
Acid value	Maximum 10	Maximum 0.5	Maximum 1
Peroxide value	Maximum 10	Maximum 5	Maximum 5

pherol. Table 1 and Figs. 1 (*a*)–1(*c*) show the compositions of these products as well as the structure of the individual components, respectively.

Phosphatidylcholine, commonly called lecithin, is neutral and a zwitterion in a broad pH-region. Fresh PC has a white colour but after contact with air it will turn brown, hygroscopic and wax-like. PC is easily dissolved in ether or alcohol (Roempp, 2012). PC can form different lyotropic phases, *e.g.* gel or liquid crystalline states depending on their derivatives and mixtures of them [1-palmitoyl-2-oleylphosphatidylcholine (POPC), dimyristoylphosphatidylcholine (DMPC), dipalmitoylphosphatidylcholine (DPPC), *etc.*] (Curatolo *et al.*, 1985). LPC, sometimes called lysolecithin, can be obtained in a catalytic process of PC involving the enzyme phospholipase A (Roempp, 2012). Tocopherols are organic compounds consisting of various methylated phenols. They are insoluble in water but soluble in fats and oils and most hydrophobic solvents. Tocopherols exist in several forms distinguished by the number of methylene groups and their positions. One form of tocopherols is α-tocopherol, which is represented in Fig. 1(*e*).

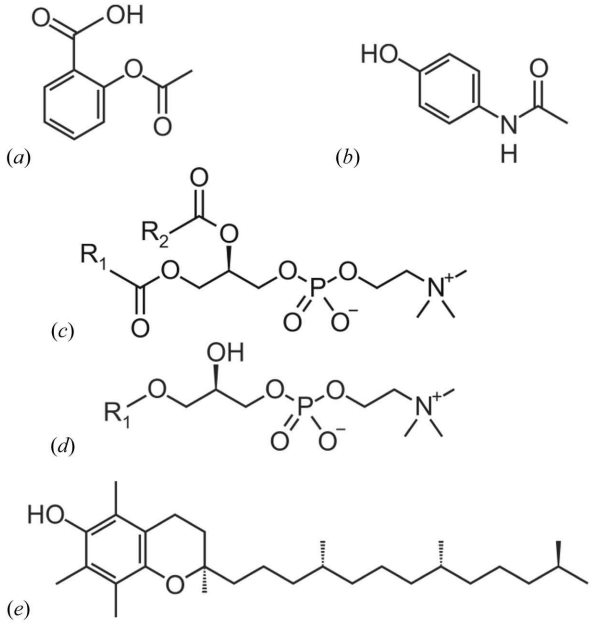

Figure 1
Chemical structures of drugs and phospholipid constituents. (*a*) Acetylsalicylic acid. (*b*) Paracetamol. (*c*) Phosphatidylcholine; R_1 and R_2 are long-chain unbranched aliphatic radicals with up to four double-bonds. (*d*) Lysophosphatidylcholine; R_1 is either acyl, alkyl or alkynyl group. (*e*) One of the most abundant forms of tocopherol (α-tocopherol).

The use of multilamellar vesicles (MLVs) has advantages in the incorporation of drugs in different places including between the layers of MLVs which may increase the drug loading. A high drug loading is important for the pharmaceutical dosage form. Furthermore, MLV can easily be prepared because no further size reduction such as by extrusion is needed. The extrusion process will also affect the structure of the liposomes. This affect was reduced in our project. Some groups also applied MLVs for study of interaction of drug and membrane (*e.g.* Barrett *et al.*, 2012).

Commercial phospholipids (PLs) were used to understand the real mechanism when these PLs were used, especially in the pharmaceutical industry, and it is thus important to understand the behaviour of these PCs in combination with drugs. Normally, pure PLs will not be used in the pharmaceutical industry since they are more expensive.

The aim of this work was to study how the nanostructure of liposomes was affected by the uptake of two common drugs, acetylsalicylic acid (ASA) and paracetamol (PA). These drugs have different properties regarding their water solubility, molecular weight or pK_a which may be important for their interaction with the liposome bilayer and thus the adsorption/absorption mechanism. The X-ray scattering technique [small- and wide-angle X-ray scattering, SAXS and WAXS, respectively] was used to determine the nanostructure of the liposomes, successfully applied in former studies (Wonglertnirant *et al.*, 2012; Gramdorf *et al.*, 2008). To analyze the experimental data, the X-ray scattering model developed by Pabst *et al.* (2000) was utilized.

2. Materials and methods

2.1. Materials

Purified phosphatidylcholine 92.0–98.0% (Phospholipon 90G, 90NG, 85G) was provided by Phospholipid GmbH (Cologne, Germany). ASA and PA were purchased from Fragron GmbH (Barsbüttel, Germany). Chloroform (Sigma Aldrich, Germany) and methanol (Merck, Germany) were of analytical grade.

Two model drugs, ASA and PA, were used in this study. ASA (Fig. 1*a*) is a white crystalline or colourless powder with a molecular weight of 180.16 g mol^{-1}. The solubility of ASA is 0.25 g in 100 ml of water at 288 K with a pK_a of 3.49 at 298 K (Gutknecht, 1992; Roempp, 2012). PA (Fig. 1*b*) has a molecular weight of 151.16 g mol^{-1}. It is a white crystalline powder with a slightly bitter taste. PA is soluble in 70 parts of water and in seven parts of alcohol. The solubility of PA in water increases as the pH and the temperature increases (Granberg & Rasmuson, 1999; McLoughlin *et al.*, 2003). The pK_a for paracetamol is between 9.5 and 9.7 at 298 K (Public Assessment Report PL 20941/0002; Gutknecht, 1992; Fairbrother, 1974).

electronic reprint

2.2. Preparation of liposomes

Three types of phospholipids were used to prepare the liposomes, *i.e.* Phospholipon 85G, 90G and 90NG (referred as 85G, 90G and 90NG, respectively). Liposomes were prepared by the thin-film hydration method. Briefly, the phospholipid (2×10^{-5} mol) was dissolved in 100 µL of a chloroform/methanol mixture (2:1, *v*/*v*) and then the organic solvent was evaporated under vacuum condition at 313 K for at least 24 h. The material became dry and the thin-film was observed at the bottom of a glass vial. The hydration phase was performed by adding 1 ml of sterile water and mixed by a vortex until the thin film was completely dispersed. In the case of the thin film prepared from 90G, complete dissolution of the thin film was difficult to obtain when employing only a vortex to dissolve the film. Therefore, the suspension was heated up to 323 K for 5 min and then stirred by a vortex. These two steps (heat and vortex) were repeated alternately until the thin film was completely dissolved. Consequently, bare liposomes were prepared.

For drug-loaded liposomes different molar ratios between the phospholipid and the drug were used. The ratios between the phospholipids and the ASA used were 1:0.1 and 1:1 in both 85G and 90G. Molar ratios of 1:1 and 1:10 were applied to 90NG. The ratio 1:1 was applied to PA in 85G bilayers, and two ratios 1:0.1 and 1:1 utilized for 90G and 90NG. The preparation routine was the same as for preparation of bare liposomes. Only the hydration phase was prepared by addition of aqueous drug solution instead of sterile water. The size and size distributions of different liposomes were determined by a light microscope (Motic BA, Wetzlar, Germany) as well as by laser light scattering (Malvern, UK).

2.3. X-ray scattering measurement

The experiments were performed at beamline B1 at DORIS III, HASYLAB/DESY in Hamburg, Germany. Scattering from the sample was simultaneously collected by two detectors, one for the WAXS and one for the SAXS region to improve the resolution of the scattering spectrum in the area of interest. The WAXS signal was mainly used to control the quality of the measurements, *i.e.* the presence of precipitations or bubbles in the sample. The SAXS patterns (0.03–1 Å^{-1}) were acquired using a large-area pixel detector (PILATUS 1M, Dectris, Switzerland) with pixel size of 172 µm × 172 µm. The WAXS signal (1–4 Å^{-1}) was measured simultaneously using a Mythen strip detector (Dectris, Switzerland). The distance from the sample to the detector was 0.885 m and the X-ray energy was 14 keV.

Samples of less than 100 µL were filled into a glass capillary (Hilgenberg GmbH, Malsfeld, Germany) with a diameter of 1.5 or 2.5 mm and a wall thickness of 0.01 mm. The capillaries were sealed with epoxy resin adhesive (UHU Quickset EPOXY Resin Glue, Germany) and fixed onto a holder, which was placed into a measuring vacuum chamber. The SAXS/WAXS measurements were performed at ambient temperature (297 K). The raw scattering data were background-corrected, integrated and calibrated using a MATLAB-based analysis suite, which is available at the beamline. The scattering signal from the solvent was removed at a later stage but before the structural analysis.

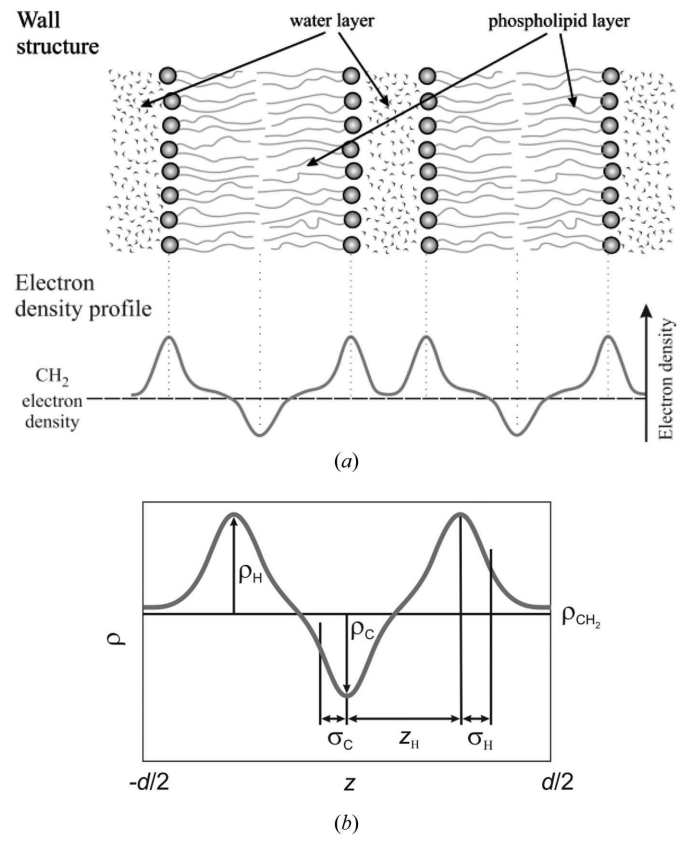

Figure 2
(*a*) Schematic representation of the electron density distribution in a lipid multilayer wall. (*b*) Electron density profile with its characterizing parameters (modified from Pabst *et al.*, 2000).

2.4. Scattering model and fitting the experimental data

The scattering model employed to capture the main features of electron density contrast across the liposome wall has been developed by Pabst *et al.* (2000) and is described in more detail in the supplementary material.[1] Briefly, the liposome wall is characterized by a multilayer structure which is picked up by X-ray scattering by the repetitive fluctuations in electron density (Fig. 2*a*). The phospholipid head-groups contain electron-rich elements like oxygen and phosphorus, resulting in higher electron density compared with the rest of the system. The tail of the phospholipid contains only hydrocarbon groups and has thus a lower electron density than the heads as well as the water that is present between the bilayers and surrounds the liposomes.

In total, nine parameters were used to fit the scattering model to the experimental data. Five of those parameters are shaping the profile of the bilayer such as: maximum and minimum densities of the head-group and chain-group,

[1] Supplementary data for this paper are available from the IUCr electronic archives (Reference: CO5031). Services for accessing these data are described at the back of the journal.

electronic reprint

respectively (ρ_H and ρ_C), broadness of the Gaussian distribution representing the head- and chain-groups (σ_H and σ_C), and the distance between the centre of the bilayer and the centre of the head-group (z_H). Other parameters are the repetitive distance between bilayers (d), number of bilayers in the wall (N), the Caillé parameter (η) describing mechanical stress in the layer caused by bending, and an additional diffusive scattering term (N_{diff}) representing the influence of wall defects and fluctuations to the total scattering.

The calculated scattering curves were fitted to the experimental data in reciprocal space by optimizing all the variables. The fitted q-range was $0.03 \leq q \leq 0.45$ Å^{-1}. The discrepancy was monitored by the sum of the root-mean-square deviations between theoretical and experimental curves at each q-value. The optimization and search for global minima were performed by the non-linear optimization routine *fmincon*. All calculations were performed using a MATLAB-based script package developed in Uppsala.

3. Results

3.1. Fitting parameters

The calculated geometrical and structural parameters recovered from the fitting procedure are given in Tables 2–4 and the bilayer profile is schematically presented in Fig. 3. Examples of the fittings and the obtained fitting parameters are presented in the supplementary material (Fig. S1, Tables S1–S3). The most important parameters for the shaping of the scattering profile were the repetitive distance d, the head-to-mid-layer distance z_H, and the broadness of the chain-group σ_C and head-groups σ_H. The other parameters mainly affected the heights of the two diffraction peaks located around 0.1 Å^{-1} and 0.2 Å^{-1}. The diffusion term N_{diff} had the smallest influence on the fitting results.

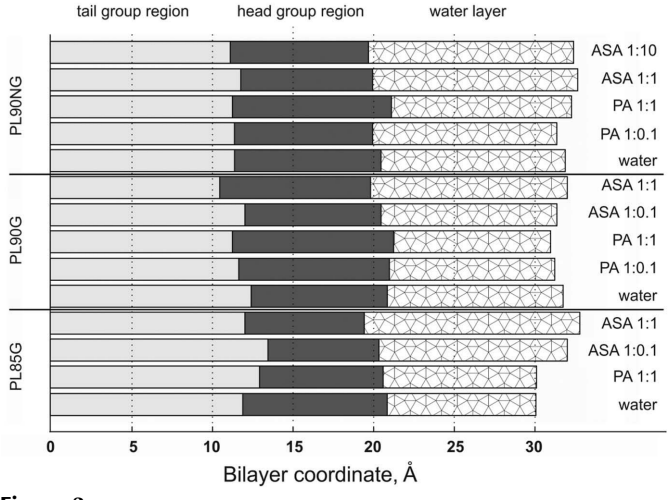

Figure 3
Half of the bilayer profile for different kinds of phospholipids. The left-hand border is matched to the centre of the bilayer and the right-hand border to the centre of the water layer. Data from bottom to top are organized according to the drug loaded to the certain phospholipid in molar ratio (*e.g.* 1:1): no drug (water), paracetamol (PA) and acetylsalicylic acid (ASA).

Table 2
Calculated bilayer structural parameters for different types of bare liposomes in water.

	85G	90G	90NG
Numbers of analyzed curves	7	5	7
Average number of layers in wall, N	2 ± 1	9.6 ± 2	9.8 ± 2
Repetitive distance, d (Å)	60.1 ± 0.2	63.4 ± 0.3	63.8 ± 0.6
Thickness of water layer, d_{water} (Å)	18.3 ± 2.8	21.8 ± 1.9	22.9 ± 2.3
Bilayer thickness, $d_{bilayer}$ (Å)	41.8 ± 2.6	41.6 ± 1.6	40.8 ± 1.7
Size of head-group, d_H (Å)	9.0 ± 0.8	8.4 ± 0.5	9.0 ± 0.5
Length of chain, d_C (Å)	11.9 ± 1.3	12.4 ± 0.8	11.4 ± 0.9
Area per lipid, A (Å^2)	61.6 ± 0.6	64.9 ± 0.4	64.3 ± 2.2

3.2. Effect of phospholipid type

The profiles of bare liposomes were taken as reference structures in the comparison with drug-loaded liposomes. Several scattering patterns were collected for each phospholipid to increase the signal-to-noise level. The structural parameters obtained from bare liposomes are shown in Table 2. The parameter that showed the largest variation was the one that represented the number of bilayers in the liposome walls, about ten bilayers for 90G and 90NG whereas only two in 85G.

The size of the head-groups was determined to approximately 9 Å in all samples with bare liposomes, consistent with previous studies by X-ray scattering and other techniques (Pabst *et al.*, 2000; Nagle & Tristram-Nagle, 2000; Gudmand *et al.*, 2009). Similar numbers have been reported for 1-palmitoyl-2-oleoyl-*sn*-glycero-3-phosphocholine layers (Pabst *et al.*, 2000) which have the same head-group structure. The length and the packing of the tails are known to vary in different kinds of liposomes (Nagle & Tristram-Nagle, 2000) and here we report values of the order of 11–14 Å which is reasonable for mixtures of natural phospholipids (Nagle & Tristram-Nagle, 2000). The electron densities of the head-group and the tail region found in this study are also consistent with previous reports (Pabst *et al.*, 2000; Lipfert *et al.*, 2007). An interbilayer thickness of 18–23 Å is also in good agreement with previous reports (Pabst *et al.*, 2000; Nagle & Tristram-Nagle, 2000) even though this thickness is somewhat dependent on the exact preparation routine.

3.3. Effect of different drugs, *i.e.* ASA and PA

Tables 3 and 4 summarize the structural parameters refined from X-ray scattering experiments and Fig. 4 shows the bilayer structure obtained from the fitting. In general, the number of bilayers in the drug-loaded liposomes was larger compared with bare liposomes. The repetitive distance and interbilayer thickness were affected more than others when the drugs were introduced. There are indications that the bilayer thickness was also modified, but uncertainties in this parameter preclude from drawing a clear conclusion. Moreover, the bilayer thickness seems to be less affected in the PA-loaded liposomes.

The head-group and the chain-group regions are also perturbed differently by the drugs. However, when it comes to the concentration dependency there are some common

electronic reprint

Table 3
Calculated bilayer structural parameters for acetylsalicylic-acid-loaded liposomes.

	85G	85G	90G	90G	90NG	90NG
Ratio of lipid to drug	1:0.1	1:1	1:0.1	1:1	1:1	1:10
Numbers of analyzed curves	2	3	2	3	5	2
Average number of layers in wall, N	10 ± 1	10 ± 1	12 ± 1	10 ± 1	7 ± 1	5.5 ± 1
Repetitive distance, d (Å)	64.0 ± 0.2	65.6 ± 0.1	62.6 ± 0.1	63.9 ± 0.1	65.3 ± 0.1	64.8 ± 0.1
Thickness of water layer, d_{water} (Å)	23.4 ± 1.0	26.6 ± 0.4	21.7 ± 0.8	24.3 ± 0.5	25.5 ± 0.3	25.3 ± 0.7
Bilayer thickness, $d_{bilayer}$ (Å)	40.5 ± 0.7	39.0 ± 0.4	40.9 ± 0.8	39.7 ± 0.5	39.8 ± 0.3	39.5 ± 0.7
Size of head-group, d_H (Å)	6.8 ± 0.5	7.4 ± 0.1	8.5 ± 0.1	9.4 ± 0.3	8.1 ± 0.1	8.6 ± 0.2
Length of chain, d_C (Å)	13.5 ± 0.4	12.1 ± 0.2	12.0 ± 0.4	10.5 ± 0.3	11.8 ± 0.2	11.1 ± 0.3
Area per lipid, A (Å^2)	68.2 ± 1.3	67.7 ± 0.6	64.0 ± 2.2	64.4 ± 0.9	64.3 ± 1.0	65.5 ± 1.9

Table 4
Calculated bilayer structural parameters for paracetamol-loaded liposomes.

	85G	90G	90G	90NG	90NG
Ratio of lipid to drug	1:1	1:0.1	1:1	1:0.1	1:1
Number of analyzed curves	3	2	3	1	2
Average number of layers in wall, N	2 ± 1	10 ± 1	9 ± 1	7 ± 1	9 ± 1
Repetitive distance, d (Å)	60.2 ± 0.3	62.4 ± 0.1	61.9 ± 0.1	62.6 ± 4.5	64.5 ± 0.1
Thickness of water layer, d_{water} (Å)	19.1 ± 1.3	20.4 ± 0.5	19.4 ± 0.8	22.8 ± 7.0	22.3 ± 0.4
Bilayer thickness, $d_{bilayer}$ (Å)	41.1 ± 1.0	42.0 ± 0.5	42.5 ± 0.7	39.8 ± 2.5	42.2 ± 0.3
Size of head-group, d_H (Å)	7.7 ± 0.6	9.4 ± 0.2	10.0 ± 0.2	8.5 ± 0.2	9.8 ± 0.1
Length of chain, d_C (Å)	12.9 ± 0.5	11.6 ± 0.2	11.2 ± 0.4	11.4 ± 1.2	11.2 ± 0.2
Area per lipid, A (Å)^2	65.2 ± 2.4	61.5 ± 1.0	60.2 ± 1.4	68.9 ± 1.1	61.5 ± 0.8

features like the thickness of the head-group layer which increases with concentration and the thickness of the chain-group region which decreases with drug concentrations. The head-group region is smaller in liposomes 85G and 90NG but broader for liposome 90G, while the opposite is seen for the chain-group. The thickness of the lipid bilayer for PA-loaded liposomes exhibits complex behaviour, resulting in a thicker bilayer for 90G and 90NG (1:1) liposomes, but thinner for others compared with the bare liposomes. The broadness of the head-group follows the same trend as the thickness of the lipid bilayer while the thickness of the chain region shows the opposite trend. For all ASA samples the thickness of the lipid bilayer is smaller compared with the bare ones.

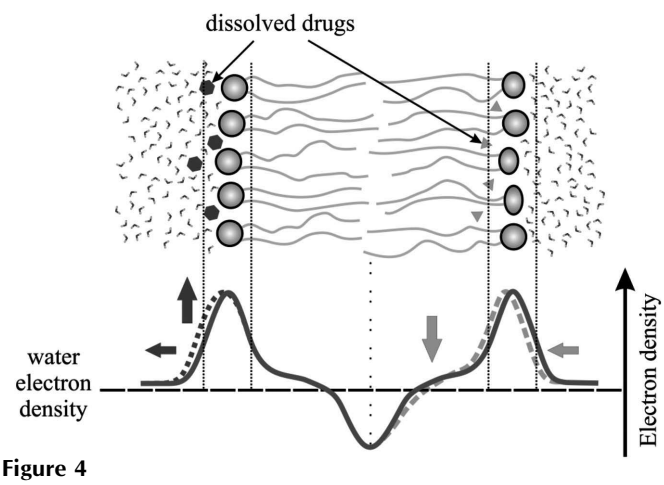

Figure 4
Schematic representation of the possible drug localization in the lipid membrane. Triangles indicate drug molecules located in the border between the head-group and the tail-group; hexagons indicate drug molecules preferably sitting on top of the lipid bilayer. The lower image shows a drug-induced change in the electron density profile. Vertical dashed lines indicate borders of non-disturbed head-group layer. Arrows indicate a drug-induced shift of the electron density profile.

4. Discussion

4.1. Structure of the liposome walls

Lipids can exist in different lyotropic phases depending on water content, *e.g.* fluid lamellar, inverse hexagonal and inverse bicontinuous cubic phases. The force that can act on the lipid bilayer can be divided into repulsive forces (*i.e.* electrostatic, steric and hydration) and attractive forces (*i.e.* hydrogen bonding, van der Waals and hydrophobic). The non-specific binding can be an advantage as a reservoir of drug because the drug will be bound within a membrane and the release of the drug can be sustained over a period of time (Seddon *et al.*, 2009). In general, the driving forces for drug adsorption and binding are hydrophobicity, electrostatic and hydrogen bonding. If both the drug and membrane are charged, electrostatic interactions are dominant, leading to non-linear binding curves. The concentration of the drug near the membrane interface can be much larger than its bulk concentration. If the drug has many conformation states, such as a random coil or an α helix, the conformation can change after binding with the lipid membrane (Seelig, 2004).

The overall size of a liposome may in general be affected by the introduction of a drug. The liposome size was therefore determined in our samples by light scattering and light microscopy. The multilamellar liposomes formed in the samples all had similar size distributions. The average size of the vesicles was in all formulations about 4 μm determined by light scattering. In control measurements by microscopy an average size of 3 μm was found. The difference between the

electronic reprint

two techniques may be related to a limited sampling of the liposomes in the latter case. In any case, the curvature of the walls is just weakly dependent on the diameter of such large liposomes so the X-ray scattering measurements will be quite insensitive for a moderate variation in the liposome sizes.

The thickness of the walls is mainly determined by the number of bilayers. In fact, the 85G-based liposome, which contains up to 10% of fatty acid in its composition (Table 1), will form large unilamellar vesicles (LUVs) or MLVs with a smaller number of layers, owing to a repulsive electrostatic interaction between the surface charged monolayers, whereas 90G and 90NG preferentially form MLVs with about ten layers. Tocopherol exists only in small amounts (less than 0.3 wt%) in the commercial PLs. Therefore it should not play any role in the thermodynamic liposome self-assembling, though it is amphiphilic.

Obtained values of the Caillé parameter for bare liposomes (Table S1 in the supplementary material) suggest that liposomes 85G and 90G have quite high levels of fluctuations which may indicate low stability of liposomes. Indeed, bare 85G liposomes have on average two layers in the wall, which indicates that the sample is probably a mixture of single-walled vesicles and MLVs. On the other hand, bare 90G liposomes form MLVs; therefore, the high value of the Caillé parameter could be the fingerprint of impurities in the structure of liposomes. The Caillé parameter for liposomes 90NG correlates with previous literature data for 1-palmitoyl-2-oleoyl-*sn*-glycero-3-phosphocholine (Pabst *et al.*, 2000).

The loading of the drugs affects the number of bilayers, where a change in the number of bilayers is particularly pronounced in 85G loaded with ASA. In this case the number of bilayers increased from two to about ten (Tables 2 and 3). In 90G the effect is much smaller and in 90NG the number of bilayer actually decreases. For liposomes loaded with PA we see a completely different behaviour in 85G where the number of bilayers is not affected at all. Obviously ASA has a stronger influence than PA on the formation and stability of multilayered liposomes of the 85G type. The data from Table 3 show that a positively charged drug ASA (pK_a 3.49) must interact with the surface charge of the 85G-based liposome, favouring MLVs formation as observed by the increase in the number of bilayers. On the other hand, an uncharged drug PA (pK_a ~9–10) did not promote multilayers formation in 85G-based liposome (Table 4).

The data acquired from drug-loaded liposomes indicate that the Caillé parameter decreases in value for liposomes 85G and 90G and increases for 90NG compared with bare liposomes. The two exceptions, however, are ASA-loaded 85G liposomes at 1:0.1 molar ratio and PA-loaded 90NG liposomes at 1:0.1 molar ratio. However, the relative error in these two cases is also high, exceeding 30%. Moreover, the scattering signal for PA-loaded 90NG liposomes at 1:0.1 ratio is very weak which increases uncertainties in parameter determination.

A further increase of the drug concentrations tends to reduce the number of bilayers and the thickness of the wall. There is one exception, however, seen for PA in 90NG where a small increase of the thickness is observed. Whether this anomaly is real or not cannot be conclusively confirmed within the accuracy of the modelling. A drug concentration dependency on bilayer stability has previously been observed for red blood cells (Schreier *et al.*, 2000). In this study the red blood cells were stabilized by low drug concentration, while high drug concentration destabilized the cell membrane. Further investigations may help to clarify the origin of the effect, while the effect itself could have practical applications. The drug concentration may be used to manipulate the structure of vesicles and helping to design vesicles with given properties.

4.2. Interbilayer and bilayer structure

Our data show that the interbilayer, *i.e.* the water layer between the bilayers, and bilayer thickness are influenced differently by the two drugs tested here (Tables 2–4, Fig. 3). The interbilayer spacing is in general larger and the bilayers thinner in ASA-loaded liposomes compared with bare liposomes. This effect becomes more pronounced at higher concentrations. The PA-loaded liposomes show quite the opposite trend: higher PA concentration makes the water layer between the bilayers thinner and the bilayer thicker. The variation in the water layer thickness may be explained by a model assuming strong bilayer–bilayer interaction introduced by Gordeliy *et al.* (1998). According to this hypothesis, the bilayer equilibrium distance is determined by repulsive short-range forces and attractive long-range van der Waals forces. The bilayer surface polarizes the interbilayer solvent molecules which will affect the equilibrium structure, which in turn induces a repulsive potential between the neighbouring bilayer. The repulsive potential between the bilayers is solvent-dependent where the size of the solvent molecules becomes important. Admixture of a drug molecule results in a higher repulsion of the bilayers which increases the thickness of the water layer. The change of the water layer profile in the ASA-loaded systems may be explained by such a bilayer–solvent–bilayer interaction. In the case of PA-loaded liposomes the hypothesis could be applied only to liposome 85G owing to similarities in the structure of this sample with ASA-loaded liposomes.

A previous study of phospholipid multilamellar membranes shows that ASA can localize at the head-group of the DMPC lipid and stabilize this region (Barrett *et al.*, 2012). Moreover, ASA can increase permeability and fluidity, as well as flexibility of the membrane. In contrast, cholesterol localizes in the hydrophobic core and increases rigidity as well as reducing the permeability of the membrane (Barrett *et al.*, 2012). Similar results were found by Casal *et al.* (1987). The interaction of ASA with the DPPC bilayer was investigated. The temperature of the main gel-to-liquid-crystal phase transition as well as the pretransition temperature of DPPC was markedly reduced in the presence of the drug. The interaction of ASA (pH < pK_a) with DPPC was limited to the polar head-group which caused an increase of hydration and head-group volume. The drug did not embed in the hydrocarbon core. If the drug ASA was ionized (pH > pK_a) it did not interact with DPPC. Lichtenberger *et al.* (2012) found that ASA in an

electronic reprint

uncharged state (pH < pK_a) will localize at the alkyl tail region, whereas the anionic form of ASA (pH > pK_a) preferred to stay towards the head-group due to the electrostatic interactions. Aspirin can significantly increase the conductance of the membrane from phosphatidylcholine. This occurrence may be explained by the protonation of ASA at low pH as well as the weak acid anion at neutral pH (Gutknecht, 1992). This is in contrast to salicylate, which is an active metabolite of ASA, and is a small amphiphilic molecule. Salicylate can disrupt membrane stability by decreasing membrane stiffness and membrane thickness. Salicylate is composed of a non-polar benzene ring and a polar domain consisting of carboxyl and hydroxyl groups. This amphiphilic structure points out that salicylate will penetrate into the lipid membrane and alter the physical properties. Salicylate exists as dimers in solution and is able to induce the micellar chain formation. Salicylate can decrease the hydrophobicity of the membrane layer and therefore caused a more wettable membrane because of higher hydrophilicity or an increase in the permeability of the membrane. Salicylate can induce the formation of membrane pores as well as stabilize the holes (Zhou & Raphael, 2005). Salicylate anions (pH > pK_a) can adsorb to the bilayer and produce a negative electrostatic surface potential which would modify the interfacial ion concentrations and thus give rise to changes in permeability. The study was performed with the neutral and amphoteric lipid phosphatidyl ethanolamine (McLaughlin, 1973). If a drug (*e.g.* salicylate) can form the internal hydrogen bond between carboxyl and the hydroxyl group, this bond will delocalize the negative charge, and thereby increase the permeability and conductance of the anion. The location of the hydroxyl group on the benzene ring has a crucial effect on the permeability of the drug (Gutknecht, 1992). Another analgesic drug, *i.e.* diclofenac, caused an increase in rigidity in the polar head-group of the model membranes and an increase of the disorder of the hydrocarbon chains (Seddon *et al.*, 2009). Paracetamol was found to have low permeability because of its high pK_a (Gutknecht, 1992). Guilmin *et al.* (1982) explained that the positively charged drug can interact with the anionic lipid membrane by the electrostatic interaction. The drug interacts with the lipid depending on the charge, the component as well as the physical state of the lipid. For example, the drug tetracaine can penetrate into the cardiolipin-lipid core. On the other hand, adriamycin has a very high affinity for cardiolipin but did not penetrate into the lipid core. Therefore, adriamycin can stabilize the complex between drug and lipid.

However, our systems have water layers in between the lipid bilayers where the drugs are dissolved. Our data indicate that the charged ASA may not only stay on the polar head-group but also be present in the lipid membrane which can be confirmed by an increase in repetitive distance, water layer thickness, length of chain and area per lipid. An increase of ASA in the water layer would also affect the ASA concentration in the membrane. In X-ray scattering, this should be reflected as a broadening of the head-group region since ASA has higher electron density with respect to water. This is visible in our data for all the phospholipid types.

Similar to ASA and 85G, PA can reduce the size of the head-group but increase the length of the chain and area per lipid, which may indicate the interaction of the uncharged drug PA with the charged lipid. This interaction, however, may be different than that of ASA; in contrast, the interaction of the uncharged drug PA with the uncharged lipid (90G and 90NG) was different to that with ASA. Concentrations of the drug PA have an effect on the parameters. Fig. 4 shows the possible localization of a drug, which can be on the head-group, between the tails or both. The localization of a drug is dependent on its water solubility, its charge status as well as the charge status of the lipid membrane.

5. Conclusions

In this work we investigated the effect of acetylsalicylic acid and paracetamol on the nanostructure of liposomes prepared from commercially available phospholipid mixtures. X-ray scattering was employed to monitor the drug-induced structural rearrangements in the lipid bilayers and interbilayer environment. Even though the experimental data reveal a complicated picture of the drug–bilayers interaction, they clearly show how the bilayer structure is affected when the liposomes are loaded with paracetamol and acetylsalicylic acid at different concentrations. The addition of ASA seems to favour the formation of multilamellar walls compared with the unloaded liposomes in 85G. In addition, it caused an increase of the repetitive distance, water layer thickness, length of chain and area per lipid but reduced the size of head-group and bilayer thickness. The effect of paracetamol was less pronounced, and the changes of these parameters were negligible in 90G and 90NG or sometimes in the opposite way.

The authors are grateful to beamline scientist Dr Ulla Vainio for experimental support as well as scientists H. Bilek and L. Tong and all the students (especially M. Herbeck) of the Beuth Hochschule für Technik Berlin for the experimental help. We also express our thanks to Adrian Rennie (Uppsala University, Department. of Physics and Astronomy) for valuable discussions. The work was supported by the Swedish Science Research Council (VR), C. F. Liljewalchs foundation and DESY by providing beam time and travelling support grants.

References

Barrett, M. A., Zheng, S., Roshankar, G., Alsop, R. J., Belanger, R. K., Huynh, C., Kučerka, N. & Rheinstädter, M. C. (2012). *PLos ONE*, **7**, e34357.

Casal, H. L., Martin, A. & Mantsch, H. H. (1987). *Chem. Phys. Lipids*, **43**, 47–53.

Castorph, S., Riedel, D., Arleth, L., Sztucki, M., Jahn, R., Holt, M. & Salditt, T. (2010). *Biophys. J.* **98**, 1200–1208.

Curatolo, W., Sears, B. & Neuringer, L. J. (1985). *Biochim. Biophys. Acta*, **817**, 261–270.

Custódio, J. B., Almeida, L. M. & Madeira, V. M. (1991). *Biochem. Biophys. Res. Commun.* **176**, 1079–1085.

Drummond, D. C., Zignani, M. & Leroux, J. (2000). *Prog. Lipid Res.* **39**, 409–460.

electronic reprint

Fairbrother, J. E. (1974). *Analytical Profiles of Drug Substances*, Vol. 3, pp. 1–109. New York/London: Academic Press.

Gallois, L., Fiallo, M. & Garnier-Suillerot, A. (1998). *Biochim. Biophys. Acta*, **1370**, 31–40.

Gordeliy, V. I., Kiselev, M. A., Lesieur, P., Pole, A. V. & Teixeira, J. (1998). *Biophys. J.* **75**, 2343–2351.

Gramdorf, S., Hermann, S., Hantschel, A., Schrader, K., Müller, R. H., Kumpugdee-Vollrath, M. & Kraume, M. (2008). *Colloids Surf. A*, **331**, 108–113.

Granberg, R. A. & Rasmuson, Å. C. (1999). *J. Chem. Eng. Data*, **44**, 1391–1395.

Gudmand, M., Fidorra, M., Bjørnholm, T. & Heimburg, T. (2009). *Biophys. J.* **96**, 4598–4609.

Guilmin, T., Goormaghtigh, E., Brasseur, R., Caspers, J. & Ruysschaert, J. M. (1982). *Biochim. Biophys. Acta*, **685**, 169–176.

Gutknecht, J. (1992). *Mol. Cell. Biochem.* **114**, 3–8.

Heerklotz, H. (2004). *J. Phys. Condens. Matter*, **16**, R441–R467.

Lichtenberger, L. M., Zhou, Y., Jayaraman, V., Doyen, J. R., O'Neil, R. G., Dial, E. J., Volk, D. E., Gorenstein, D. G., Boggara, M. B. & Krishnamoorti, R. (2012). *Biochim. Biophys. Acta*, **1821**, 994–1002.

Lipfert, J., Columbus, L., Chu, V. B., Lesley, S. A. & Doniach, S. (2007). *J. Phys. Chem. B*, **111**, 12427–12438.

McLaughlin, S. (1973). *Nature (London)*, **243**, 234–236.

McLoughlin, C. M., McMinn, W. A. M. & Magee, T. R. A. (2003). *Powder Technol.* **134**, 40–51.

Molema, G. & Meijer, D. K. F. (2001). *Drug Targeting.* Weinheim: Wiley-VCH.

Nagle, J. F. & Tristram-Nagle, S. (2000). *Biochim. Biophys. Acta*, **1469**, 159–195.

Pabst, G., Rappolt, M., Amenitsch, H. & Laggner, P. (2000). *Phys. Rev. E*, **62**, 4000–4009.

Putnam, C. D., Hammel, M., Hura, G. L. & Tainer, J. A. (2007). *Q. Rev. Biophys.* **40**, 191–285.

Roempp, J. (2012). *RÖMPP*, http://www.roempp.com (1 October 2012).

Saag, M. S. & Dismukes, W. E. (1988). *Antimicrob. Agents Chemother.* **32**, 1–8.

Schreier, S., Malheiros, S. V. & de Paula, E. (2000). *Biochim. Biophys. Acta*, **1508**, 210–234.

Seddon, A. M., Casey, D., Law, R. V., Gee, A., Temper, R. H. & Ces, O. (2009). *Chem. Soc. Rev.* **38**, 2497–2812.

Seelig, J. (2004). *Biochim. Biophys. Acta*, **1666**, 40–50.

Seydel, J. K. & Wiese, M. (2002). *Drug-Membrane Interactions.* Weinheim: Wiley-VCH.

Torchilin, V. P. & Weissig, V. (2003). *Liposomes.* Oxford University Press.

Ulrich, A. S. (2002). *Biosci. Rep.* **22**, 129–150.

Wonglertnirant, N., Ngawhirunpat, T. & Kumpugdee-Vollrath, M. (2012). *Biol. Pharm. Bull.* **35**, 1–9.

Zhou, Y. & Raphael, R. M. (2005). *Biophys. J.* **89**, 1789–1801.

electronic reprint